ELSEVIER

Journal of Molecular Structure: THEOCHEM 764 (2006) 21–31

THEO CHEM

www.elsevier.com/locate/theochem

# Secondary *N*-nitrosocarbamate anions: Structure and alkylation reactions. A DFT study

Vladimir Benin *

*Department of Chemistry, University of Dayton, 300 College Park, Dayton, OH 45469-2357, USA*

Received 12 January 2006; accepted 23 January 2006
Available online 5 April 2006

**Abstract**

The current article reports theoretical studies (DFT: B3LYP/6-31+G(d)) on the structure and alkylation reactions of the anions of some secondary *N*-nitrosocarbamates, a class of ambident nucleophiles whose chemistry has been little explored. Several anions (**1**–**4**), with an increasing size of the carbamate alkyl (aryl) group were investigated, in an attempt to establish the influence of the size of that group on the thermal stability and regioselectivity of alkylation of the title anions. The conclusion is that thermal stability and the mode of reaction are affected significantly only in the presence of very large and branched carbamate groups. The thermal decomposition studies at the B3LYP/6-31+G(d) level of theory yield quantitative results that are in very good or excellent agreement with experimental data. A detailed study of *N*- vs. *O*-alkylation reactions was conducted, in an attempt to reveal the nature and origin of regioselectivity. Several factors seem to play prominent role: (1) charge distribution within the *N*-nitrosocarbamate anion; (2) exothermicity of alkylation; (3) size of electrophile and (4) size of the carbamate alkyl (aryl) group. Computational results on the alkylation reactions of *N*-nitrosocarbamate anions are compared to results for alkylation of the acetone enolate ion, the outcome for the latter being in sharp contrast to earlier, lower-level calculations. In addition, alkylation studies were conducted on the *Z*-isomers of the title anions and the results indicate that they undergo *O*-alkylation with significantly lower barriers compared to the *E*-isomers. However, *Z*-isomers are 5–6 kcal/mol less stable thermodynamically and application of the Curtin–Hammett principle leads to the conclusion that *O*-alkylation occurs almost exclusively on the *E*-isomers.


*Keywords:* *N*-nitrosocarbamates; Enolate ions; Ambident nucleophiles; Alkylation; DFT calculations

## 1. Introduction

*N*-nitrosoamides (including *N*-nitrosoureas and *N*-nitrosocarbamates) and *N*-nitrosoamines have been the object of extensive studies during the past 50 years, related to their potent carcinogenicity [1]. At the same time, some of them have proved to be very effective anti-tumor agents. Both aspects of their biological activity have provoked numerous investigations that have led to considerable broadening of the knowledge we have today on various aspects of their molecular biochemistry [2–4]. An overwhelming proportion of this voluminous body of work is devoted to the chemistry and biochemistry of tertiary *N*-nitroso compounds (*N*-alkyl-*N*-nitrosoamides and *N*-alkyl-*N*-nitrosocarbamates). Secondary *N*-nitrosocarbamates remain largely unknown. Their studies have been greatly complicated due to lower thermal stability and greater reactivity. The best-known representative of secondary *N*-nitrosocarbamates is *N*-nitrosourethane, whose preparation was originally reported in the late 19th century [5]. The compound was obtained and studied both in the neutral state and in the form of its silver, ammonium or potassium salts.

The chemistry of *N*-nitrosourethane and its salts was reinvestigated in a recent work, in which studies were conducted on the more thermally stable and easily soluble tetrabutylammonium salt, **1**-$\mathbf{NBu_4}$ [6]. The conclusion from this work was that the *N*-nitrosourethane anion **1**, in analogy to enolate anions, is a typical ambident nucleophile and undergoes alkylation reactions at three different centers, yielding mixtures of *N*-alkylated, *O*-alkylated and azoxy derivatives (Scheme 1). Alkylation reactions revealed the expected dependence of the *N*/*O*-alkylation ratio on the size of the alkyl moiety, with larger groups giving predominantly the product of *O*-alkylation, the least sterically demanding pathway. Kinetic studies of **1**-$\mathbf{NBu_4}$ and some of its *O*-alkylated derivatives, as well as computational analysis of model structures suggested that thermal decomposition of the *N*-nitrosourethane anion and its derivatives occurs by a concerted mechanism.

* Tel.: +1 937 229 4762; fax: +1 937 229 2635.
*E-mail address:* vladimir.benin@notes.udayton.edu

0166-1280/$ - see front matter © 2006 Elsevier B.V. All rights reserved.
doi:10.1016/j.theochem.2006.01.030

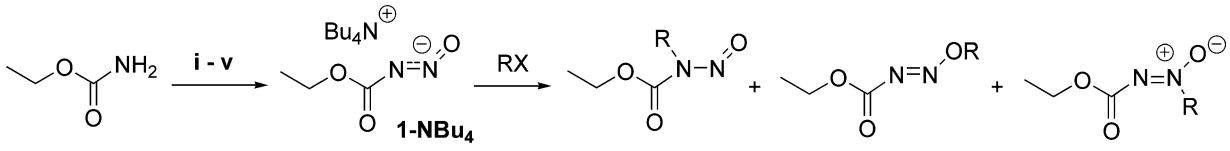


Scheme 1.

Several important questions have remained to be answered however:

(1) The role of the counter-ion for the relative stability of the *E*- and *Z*-isomeric forms of *N*-nitrosocarbamate anions.
(2) Potential influence of the size of the carbamate alkyl (aryl) group on the thermal stability of *N*-nitrosocarbamate anions.
(3) Influence of the carbamate alkyl (aryl) group on the regioselectivity of alkylation reactions, i.e. *N*- vs. *O*-alkylation.
(4) Rate of alkylation of the *E*- and *Z*-isomers of *N*-nitrosocarbamate anions and structures of the *O*-alkylated derivatives.

In order to address these questions, the computational analysis of four *N*-nitrosocarbamate anions (**1**–**4**) and their *O*- and *N*-alkylated derivatives was undertaken and we present it in the current report. Earlier theoretical studies, at the MP2 level, using the 6-31G(d) basis set, systematically underestimated energy barriers and led to kinetic parameters that deviated considerably from experimental values [6]. Hence, our decision to switch to DFT and extend the basis set for optimizations. Experimental efforts towards the preparation and isolation of the title anions have been described in a recently published work [7].

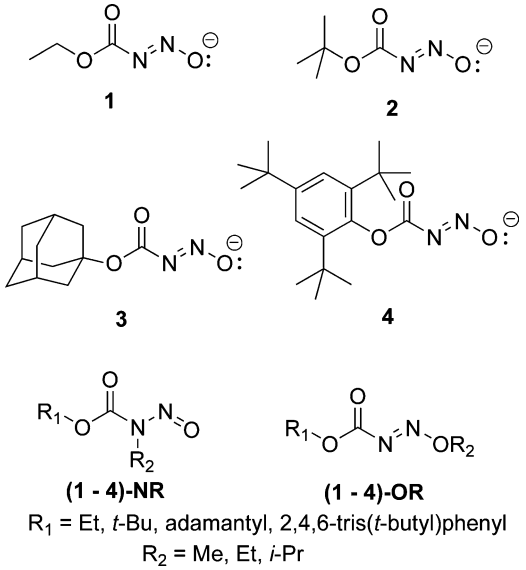


## 2. Results

### 2.1. Computational protocol

All calculations were performed using the GAUSSIAN 03/GaussView software package [8], on a Linux-operated QuantumCube QS4-2400C by Parallel Quantum Solutions [9]. Calculations, unless otherwise specified, were conducted using DFT at the B3LYP/6-31+G(d) level [10–12], taking into account the fact that for anions, the use of diffuse functions is recommended [13–16]. All calculations were performed at 298 K. All minima and transition state structures were validated by subsequent frequency calculations at the same level of theory. All minimum structures had sets of only positive second derivatives, while transition state structures all had one imaginary frequency. In some cases, the relationship of minima and connecting transition states was further verified by IRC calculations [17,18]. Transition state searches were conducted employing the Transit-Guided Quasi-Newton method (STQN, opt=qst2 or qst3), or the Berny algorithm (opt=TS) [19,20]. Values of free energy changes were obtained after frequency calculations and zero-point energy corrections. ZPE corrections were not scaled. Implicit solvent calculations were conducted using the IEF-PCM model, with acetonitrile as a solvent (solvent=acetonitrile) [21–23]. Atomic radii were derived using UFF force field (RADII=UFF).

### 2.2. Geometries of N-nitrosocarbamate anions

All studied compounds, **1**–**4**, are subject to isomerism with respect to the N–N bond, thus defining two distinct stereoisomers in each case: **E** and **Z**. The isomer **1E** has two conformational minima with respect to the N–C bond (Fig. 1):

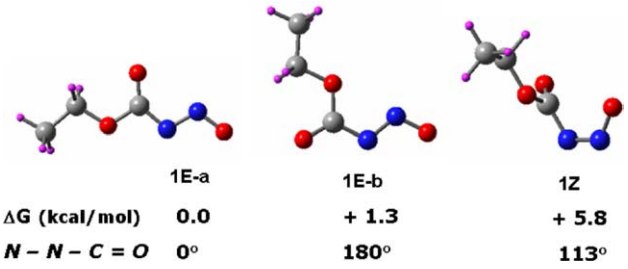


Fig. 1. Optimized geometries of conformational minima of anions **1E** and **1Z**. Relative energies with respect to the global minimum structure **1E-a**.

Table 1
Gibbs free energies of the global minima structures of the *E*- and *Z*-isomers of anions **1**–**4** and thermodynamic parameters for *E*–*Z* isomerization and thermal decomposition

| Anion | *E*-isomer | *Z*-isomer | $TS_{E-Z}$ | $TS_{Z/decomp}$ | $\Delta G_{E-Z}$ | $\Delta G^{\neq}_{E-Z}$ | $\Delta G^{\neq}_{Z/decomp}$ |
|---|---|---|---|---|---|---|---|
| **1** | −452.4629 | −452.4536 | −452.4404 | −452.4219 | **+5.8** | **+14.1** | **+19.9** |
| **2** | −531.0416 | −531.0327 | −531.0198 | −531.0005 | **+5.6** | **+13.7** | **+20.2** |
| **3** | −763.2044 | −763.1953 | −763.1828 | −763.1636 | **+5.7** | **+13.5** | **+19.9** |
| **4** | −1076.3123 | −1076.3021 | −1076.2925 | −1076.2689 | **+6.4** | **+12.4** | **+20.8** |

Gibbs free energy values (Hartrees). Gibbs free energy differences (bold values) are in kcal/mol.

**1E-a** (dihedral angle *N*–*N*–*C*=*O* = 0°), and **1E-b** (dihedral angle *N*–*N*–*C*=*O* = 180°), conformation **1E-a** being the global minimum. The anion **1Z** exists as a single conformation with respect to the N–C bond, with a dihedral angle *N*–*N*–*C*=*O* of 113°.

For all compounds **1**–**4** the *E*-isomer is lower in energy than the *Z*-isomer, with individual results listed in Table 1 (differences between global minima structures). At ambient temperature the equilibrium is significantly shifted towards the *E*-isomer, with the *Z*-isomer in all cases being present at less than 0.1%.

### 2.3. Geometries of N-nitrosocarbamate salts

Additional information is gained from further optimization studies that include counter-ions. Calculations were conducted on anion **1** in combination with either a lithium cation or a tetramethylammonium cation (Fig. 2). The *Z*-isomer actually becomes the more stable form, by 2.5 kcal/mol, when $Li^+$ is the counter ion, forming a six-membered ring through coordination of $Li^+$ to the diazotate and carbonyl oxygen centers. In the *E*-isomer, the lithium cation coordinates to the N- and O-centers, forming a four-membered cyclic chelate.

The same coordination patterns are observed with the tetramethylammonium cation but the latter is much larger, which prevents the formation of well defined, tightly bound cyclic structures. Therefore, in the tetramethylammonium salt

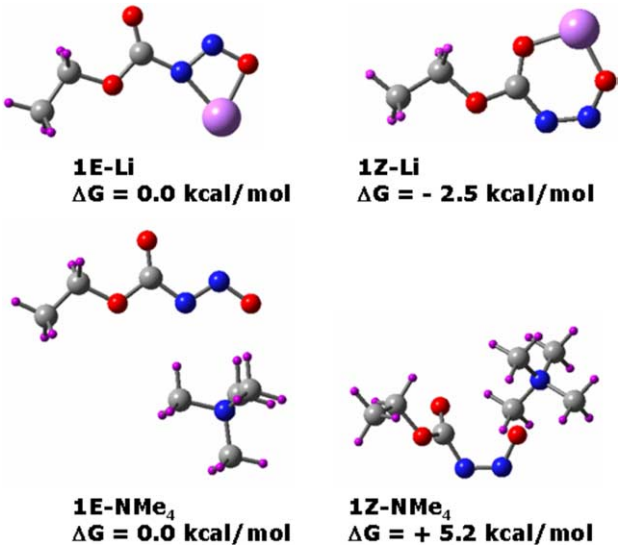


Fig. 2. Optimized geometries of the Li- and $Me_4N$-salts of anions **1E** and **1Z**. Energy differences relative to the more stable isomer in each case.

the anion resembles to a much greater extent the 'free' anion and as a result the *E*-isomer is the more stable form by 5.2 kcal/mol. These findings provide a logical explanation for the reported lower thermal stability of metal ion-containing salts of *N*-nitrosourethane [5]. In contrast to the relatively stable ammonium salt, the Na- and K-salts were reported to decompose faster and at lower temperatures. Taking into account the above-calculated conformational preferences and the fact that the *Z*-isomer is the starting structure on the thermal decomposition route (vide infra), one would expect lower stability for cases in which the anion is 'locked' in the *Z*-form.

### 2.4. E–Z interconversion

Results for the interconversion barriers are reported in Table 1. There is a gradual decrease of the barrier upon increase of the size of the ester alkyl (aryl) group. Calculations show that the *E*–*Z* interconversion does not take place by rotation around the N–N bond, but rather via a concerted process of pyramidal inversion at both nitrogen centers. The transition state structures $(\mathbf{1–4})_{\mathbf{E–Z}}$**-TS** are shown in Fig. 3, together with the optimized TS structures for *E*–*Z* interconversion of the *O*-methylated derivatives of anions **1**–**4**. Similar mechanism for isomerization has been suggested, on the basis of experimental and theoretical studies, for other N=N containing structures, such as azo compounds [24,25].

### 2.5. Thermal decomposition of N-nitrosocarbamate anions

The most favorable pathway for decomposition starts from the corresponding *Z*-isomer, as shown in Scheme 2. Two distinct routes can be suggested: (1) a concerted process, with a four-membered cyclic TS; (2) a stepwise process, with a four-membered cyclic intermediate as a distinct local minimum. Gibbs free energy values for the four anions are listed in Table 1, showing no significant increase of the barrier to decomposition upon alteration of the carbamate alkyl (aryl) group, except for anion **4**, in whose case the barrier is increased by roughly 1 kcal/mol.

The optimized TS structures are shown in Fig. 4. Selected structural parameters are explicitly listed and are very similar for all four transition states. Bond lengths indicate significant C–O bond making, while the N–N bond length is almost precisely average of those in the starting **1Z** (1.30 Å) and $N_2$ (1.10 Å). All decompositions are thermodynamically favorable, with large values of the Gibbs reaction free energy ($\Delta G < -70$ kcal/mol). The products of decomposition, in each

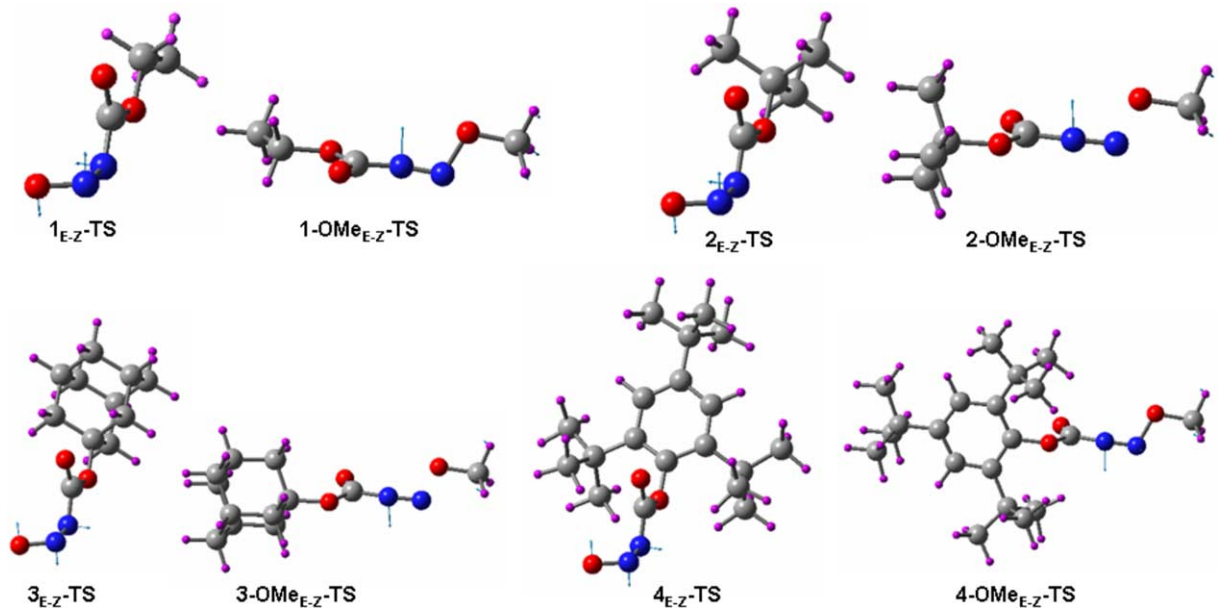


Fig. 3. Optimized transition state structures for *E–Z* interconversion of anions **1**–**4** and their *O*-methylated derivatives. Displacement vectors are shown in all cases.

case, are molecular nitrogen and the corresponding alkyl (or aryl) carbonate anion, which, in the case of compound **1**, has been experimentally observed [6].

### 2.6. N- and O-alkylation studies

As previously pointed out, the *N*-nitrosocarbamate anion is a typical ambident nucleophile, with multiple alkylation sites. The present report outlines systematic studies of alkylation at the N (C=O)-center (referred to as *N*-alkylation from this point on) as well as the nitroso *O*-center (referred to as *O*-alkylation from this point on).

Stationary points on the *N*- and *O*-methylation pathways for the **1E** and **1Z** anions are shown in Fig. 5 and numerical results are summarized in Table 2. One noticeable trend is that *N*-alkylation reactions are more exothermic than *O*-alkylations, a fact no doubt related to the greater strength of the N=O bond (BDE ~ 115 kcal/mol) compared to an N=N bond (BDE ~ 100 kcal/mol) [26]. *N*-alkylation predominates with small electrophiles, while *O*-alkylation receives greater preference with larger alkyl halides.

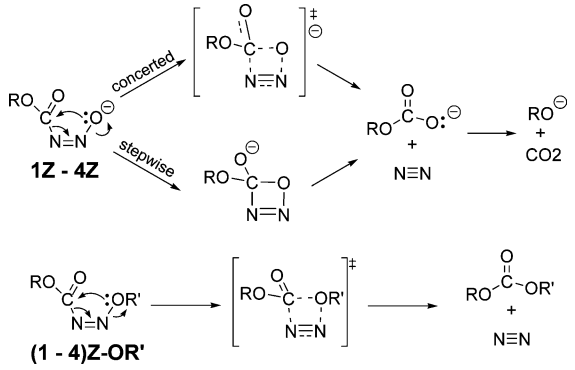


Scheme 2.

The computational results demonstrate that the thermodynamically less stable *Z*-isomer undergoes *N*-methylation and *N*-ethylation with barriers comparable to those for the *E*-isomer. Only the barrier for *N*-isopropylation is somewhat lower. For *O*-alkylations all barriers are lower for the *Z*-isomer, the difference in TS energies being 2.5 kcal/mol for methylation, 3.3 kcal/mol for ethylation and 1.9 kcal/mol for isopropylation.

Kinetic and thermodynamic data on methylation of the *E*-isomers of anions **1**–**4** are summarized in Table 3. Changing the alkyl group from ethyl (**1E**) to *t*-butyl (**2E**) does not seem to have a significant effect on the activation barriers and the effect of the 1-adamantyl group (**3E**) is only slightly more pronounced. In all those cases *N*-methylation occurs through a barrier that is 0.8–1.6 kcal/mol lower than *O*-methylation.

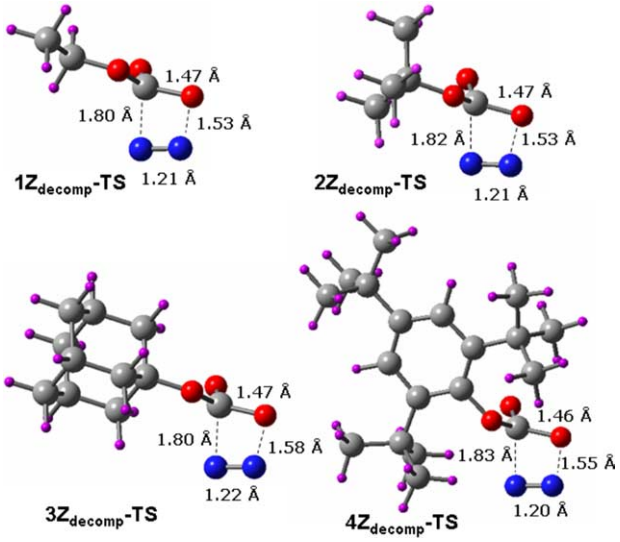


Fig. 4. Optimized four-membered cyclic transition states for thermal decomposition of anions **1Z**–**4Z**.

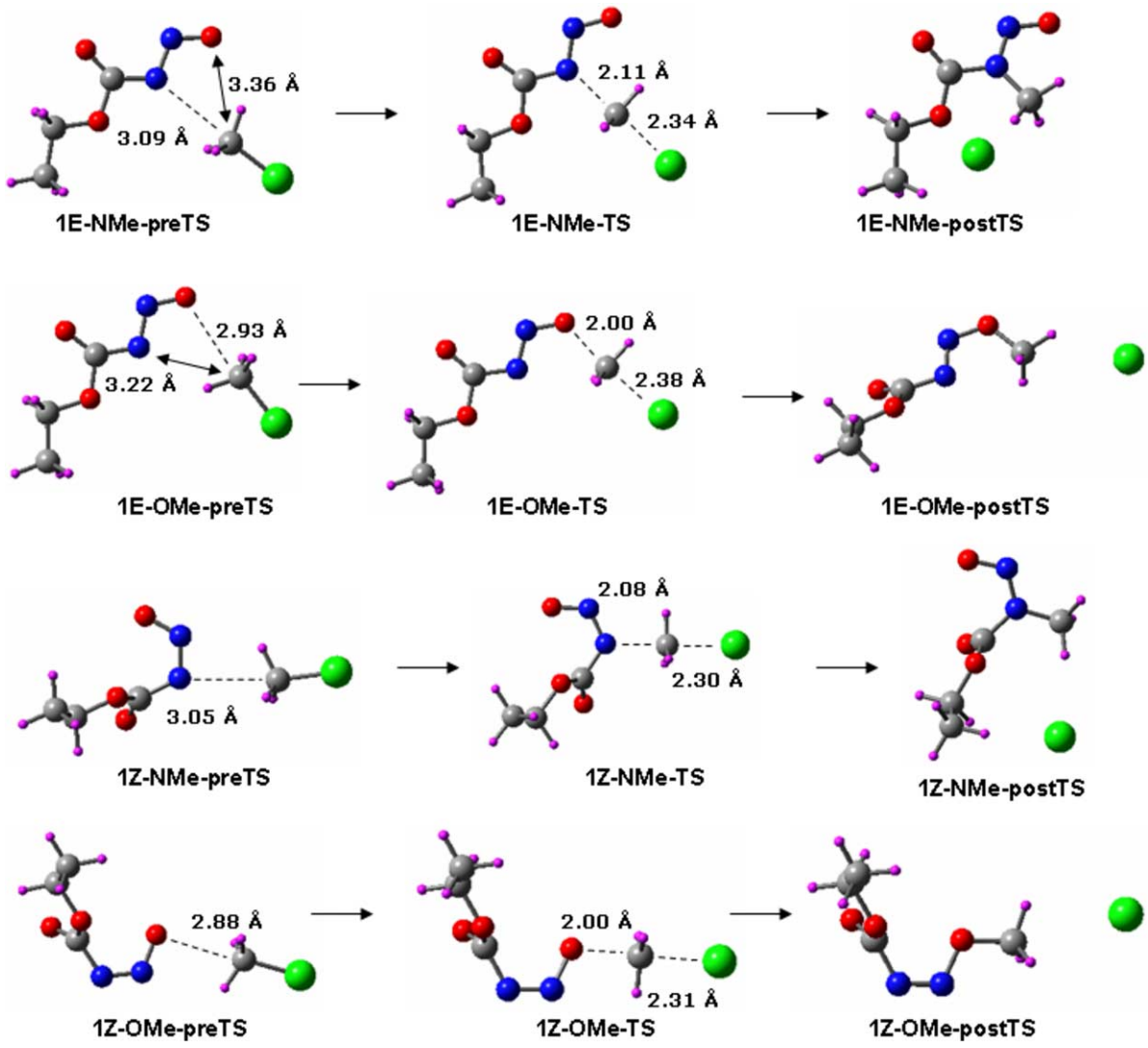


Fig. 5. Stationary points for *N*- and *O*-methylation of anions **1E** and **1Z**. $CH_3Cl$ was used as a methylating agent for all calculations.

Only in the case of the very large and branched 2,4,6-tris(*t*-butyl)phenyl group (anion **4E**) are the barriers raised more significantly. Calculations demonstrate reverse of trend in the case of **4E**, namely the barrier for *N*-methylation becomes slightly larger than the barrier for *O*-methylation. It is to be expected that in reactions with larger electrophiles (i.e. bulkier alkyl groups) the differentiation would be even more pronounced, with greater relative preference for *O*-alkylation.

### *2.7. Stability and thermal decomposition of the O-methylated derivatives, (**1**–**4**)-OMe*

Both the *E*- and *Z*-isomer of each carbamate can be *O*-alkylated, yielding (**1E**–**4E**)-**OR** and (**1Z**–**4Z**)-**OR**, respectively. Detailed analysis shows that the *E*-isomer in each case is nonplanar and exists as two distinct conformers, with different values for the dihedral angles of the carbamate core. All conformational minima of structure **1**-**OMe** are shown in Fig. 6. The conformer **1E**-**a**-**OMe** has values for the dihedral angles *N*–*N*–*C*=*O* and *C*($H_3$)–*O*–*N*–*N* of 67 and 180°, respectively, while in **1E**-**b**-**OMe** these angles are 107 and 0°. Isomer **1E**-**a**-**OMe** is the global minimum, although the two *E*-conformers are practically isoenergetic. The isomer **1Z**-**OMe** also exists as a pair of conformers, one of which is more than 10 kcal/mol higher in energy than the other.

In each case the *E*-isomer is more stable than the *Z*-isomer, but the *E*–*Z* energy differences are not as large as for the parent anions **1**–**4** (Table 4). The barriers for *E*–*Z* isomerization, on the other hand, are significantly higher, in the range of 19–21 kcal/mol. In this case too, the isomerization occurs through a pyramidal inversion at the (C=O)–*N*– nitrogen atom, rather than rotation around the N=N bond (Fig. 3).

The *O*-alkylated derivatives decompose in a fashion analogous to the starting anions, via cyclic transition states, starting from the corresponding *Z*-isomer (Scheme 1 and Fig. 7). The barriers to decomposition are 2–5 kcal/mol higher than those for the *N*-nitrosocarbamate anions **1**–**4**. Particular attention deserves **4**-**OMe**, whose calculated barrier is 25.4 kcal/mol, demonstrating the beneficial

Table 2
*N*- and *O*- alkylation reactions of anion **1**

| Alkylation reaction | **1E**[a] | | | **1Z**[b] | | |
|---|---|---|---|---|---|---|
| | Pre-TS $\Delta G$ | TS $\Delta G^{\#}$ | Post-TS $\Delta G$ | Pre-TS $\Delta G$ | TS $\Delta G^{\#}$ | Post-TS $\Delta G$ |
| *N*-methylation | −952.5601 | −952.5399 | −952.5793 | −952.5505 | −952.5283 | −952.5711 |
| | **−1.1** | **+13.1** | **−12.7** | **−0.3** | **+13.6** | **−13.4** |
| *N*-ethylation | −991.8539 | −991.8253 | −991.8673 | −991.8443 | −991.8151 | −991.8562 |
| | **−1.3** | **+17.9** | **−9.7** | **−1.1** | **+17.8** | **−8.0** |
| *N*-isopropylation | −1031.1471 | −1031.1105 | −1031.1510 | −1031.1360 | −1031.1024 | −1031.1461 |
| | **−1.9** | **+23.0** | **−4.3** | **−0.8** | **+20.3** | **−7.1** |
| *O*-methylation | −952.5607 | −952.5379 | −952.5572 | −952.5515 | −952.5329 | −952.5573 |
| | **−0.9** | **+14.3** | **+1.3** | **−0.9** | **+11.8** | **−4.5** |
| *O*-ethylation | −991.8551 | −991.8262 | −991.8511 | −991.8450 | −991.8213 | −991.8518 |
| | **−2.1** | **+18.2** | **+0.4** | **−1.6** | **+14.9** | **−5.9** |
| *O*-isopropylation | −1031.1473 | −1031.1163 | −1031.1438 | −1031.1371 | −1031.1106 | −1031.1455 |
| | **−2.0** | **+19.4** | **+0.2** | **−1.4** | **+17.5** | **−6.7** |

Gibbs free energies (Hartrees). Gibbs free energy differences (bold values) are in kcal/mol. The Gibbs free energy difference $\Delta G_{\mathbf{E-Z}} = +5.8$ kcal/mol.
[a] $\Delta G$ values are relative to the sum energy of (**1E** + alkyl halide).
[b] $\Delta G$ values are relative to the sum energy of (**1Z** + alkyl halide).

influence of the sterically congested aryl functionality on thermal stability.

Selected bond lengths of the optimized TS structures are shown in Fig. 7. Compared to the decomposition of the parent anions, the N–N bond length is even closer to that of the product $N_2$, but the C–O bond making and the C–N bond breaking lag behind. The four transition states exhibit similar sets of structural parameters.

## 3. Discussion

At present, experimental data are available for anion **1** and some of its alkylated derivatives [6], and anion **4** [27]. Effort has been made, in the following discussion, to compare calculated and experimental results, in an attempt to explore the extent of agreement between the two.

### *3.1. Stability and thermal decomposition of N-nitrosocarbamate anions **1–4** and their O-methylated derivatives*

The pathway outlined in Scheme 2, via four-membered cyclic transition state, would lead to clean fragmentation of anions **1Z–4Z** into the corresponding monoalkylcarbonate anions and $N_2$. The anion gradually decomposes further to give the corresponding alkoxide or phenoxide anion, and they have been documented by NMR in the cases of thermal decomposition of **1** [6] and **4** [27]. The barriers to decomposition show little dependence on the alkyl (aryl) carbamate group, with activation energy values around 20 kcal/mol for **1Z–3Z** and about 1 kcal/mol higher for **4Z**. Apparently, the fact that a single oxygen atom approaches and binds to the carbonyl group makes the process relatively insensitive towards the steric effect of the carbamate alkyl (aryl) group. Theoretical and experimental results are in good agreement for anions **1** and **4**. Using variable temperature NMR, anion **1** was found to decompose with a unimolecular rate constant $k_{obs} = 18.5 \times 10^{-5}$ s$^{-1}$ at 35 °C and $34.5 \times 10^{-5}$ s$^{-1}$ at 40 °C ($CD_2Cl_2$) [6]. The calculated values, assuming fast *E–Z* pre-equilibrium, are $0.4 \times 10^{-5}$ and $0.8 \times 10^{-5}$ s$^{-1}$ at the same temperatures. Using the same technique, anion **4** was found to decompose with a unimolecular rate constant $k_{obs} = 2.0 \times 10^{-5}$ s$^{-1}$ at 45 °C (in DMF-$d_7$) [27], while the calculated value at the same temperature is $0.1 \times 10^{-5}$ s$^{-1}$. For both anions the gas-phase calculated values are about an order of magnitude lower, compared to the values in solution,

Table 3
*N*- and *O*- methylation reactions of *N*-nitrosocarbamate anions **1E–4E**

| Anion | *N*-methylation | | | *O*-methylation | | |
|---|---|---|---|---|---|---|
| | Pre-TS **$\Delta G$** | TS **$\Delta G^{\neq}$** | Post-TS **$\Delta G$** | Pre-TS **$\Delta G$** | TS **$\Delta G^{\neq}$** | Post-TS **$\Delta G$** |
| **1E** | −952.5608 | −952.5399 | −952.5793 | −952.5607 | −952.5379 | −952.5572 |
| | **−1. 1** | **+13.1** | **−12.7** | **−1.1** | **+14.5** | **+1.3** |
| **2E** | −1031.1388 | −1031.1174 | −1031.1601 | −1031.1386 | −1031.1156 | −1031.1369 |
| | **0.0** | **+13.1** | **−13.4** | **+0.1** | **+14.7** | **+1.2** |
| **3E** | −1263.3011 | −1263.2146 | −1263.3235 | −1263.3008 | −1263.2775 | −1263.2963 |
| | **+0.3** | **+14.8** | **−13.5** | **+0.5** | **+15.6** | **+3.3** |
| **4E** | −1576.4080 | −1576.3792 | −1576.4135 | −1576.4080 | −1576.3799 | −1576.3971 |
| | **+0.3** | **+18.6** | **−3.2** | **+0.3** | **+18.2** | **+7.1** |

Gibbs free energy values (Hartrees). Gibbs free energy differences (bold values) are in kcal/mol. $\Delta G$ values for the pre- and post-TS minima are referenced to the sum energy of (**1-4E** + $CH_3Cl$).

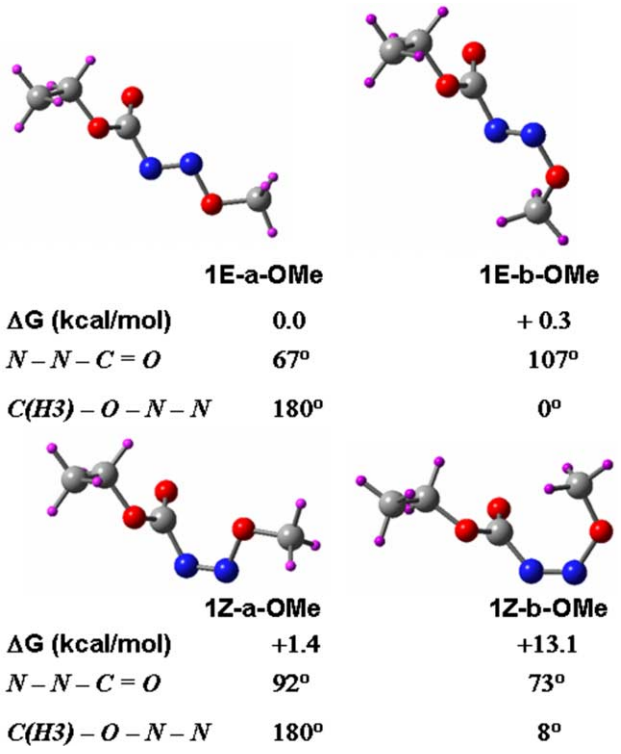


Fig. 6. Optimized geometries of conformational minima of **1-OMe**, with respect to the C(=O)–N, N=N and N–O bonds. Relative energies (kcal/mol) with respect to the global minimum **1E-a-OMe**.

corresponding to a calculated-experimental barrier differences of about 1–1.5 kcal/mol.

The influence of the carbamate alkyl (aryl) group on the barrier to decomposition is greater in the case of the *O*-alkylated derivatives. For *O*-methylation, values range from 21.5 kcal/mol for **3-OMe** to 25.4 kcal/mol for **4-OMe**. Table 4 also lists data for **1-OEt**, as it was interesting to compare the theoretical and the available (in this case experimental) value for the rate constant of decomposition. According to variable temperature NMR analysis, **1-OEt** decomposes with a unimolecular rate constant $k_{obs} = 1.77 \times 10^{-5}\ s^{-1}$ at 35 °C ($CD_2Cl_2$) [6]. The calculated value is $2.80 \times 10^{-5}\ s^{-1}$ at the same temperature, and is in excellent agreement with experiment. In general, it is anticipated that the gas-phase calculations would be in a better agreement with experimental data in the case of the neutral *O*-alkylated derivatives, compared to the charged anions **1**–**4** (or their salts), where solvation effects are expected to play a more prominent role.

A question that required resolution was the existence of a cyclic intermediate as a distinct minimum on the potential energy surface for decomposition of anions **1**–**4**. Such intermediate is shown in Scheme 2 as part of an alternative, stepwise decomposition route, and is similar to species that have been proposed to play role in the thermal decomposition of other, closely related structures, such as *N*-nitrosoamides [28,29]. Attempts to locate and optimize such an intermediate were not successful for any of the studied anions, as appropriately distorted input structures invariably collapsed into the corresponding *Z*-isomers. An IRC calculation [17,18], starting with $\mathbf{1Z_{decomp}}$-**TS**, with 31 steps in each direction, connects unambiguously the transition state to the starting anion **1Z** on one side and the final products of decomposition on the other (Fig. 8). Hence we conclude that at the current level of theory, and in agreement with earlier theoretical results [6], the thermal decomposition of anions **1**–**4** seems to be a concerted process.

We focused also on the search for alternative routes to decomposition, specifically ones that would originate from the more thermally stable *E*-isomers of the title anions. A transition state was located for the process of heterolytic cleavage of the N–O bond in compound **1E-OMe**, as shown in Scheme 3.

The N–O cleavage apparently triggers a concerted breaking of several bonds leading to the complete dissociation of the molecule into small fragments: $CH_3O^-$, $N_2$, $CO_2$ and $CH_3CH_2^+$. NBO charges (italicized figures in parentheses in Scheme 3) show an increase of the negative charge on the methoxy oxygen center and an increased positive charge on the $C(H_2)$-center in the transition state. In addition, the dihedral angle changes from $\theta = 32°$ in **1E-OMe** to $\theta = 16°$ in the transition state, as would be expected for a forming carbocationic center. This heterolytic cleavage process is, however, a non-competitive route to decomposition, since its energy barrier in the gas phase is $\Delta G^{\neq} = 50.4$ kcal/mol. Implicit introduction of solvent, using the IEF-PCM model, does lead, as expected, to a significant reduction of the barrier to $\Delta G^{\neq} = 33.3$ kcal/mol, still much higher than the barrier for concerted decomposition of **1Z-OMe**. Due to differential stabilization by the solvent, the transition state in acetonitrile, compared to gas phase, is earlier and tighter, as clearly evidenced by the differences in the distances of the breaking bonds (Table 5) and dihedral angle values (Scheme 3). Overall,

Table 4
*O*-alkylated derivatives of carbamate anions **1**–**4**

| Derivative | *E*-isomer | *Z*-isomer | $TS_{E/Z}$ | $TS_{Z/decomp}$ | $\Delta G_{E/Z}$ | $\Delta G^{\#}_{E/Z}$ | $\Delta G^{\#}_{Z/decomp}$ |
|---|---|---|---|---|---|---|---|
| **1-OMe** | −492.2625 | −492.2602 | −492.2293 | −492.2239 | **+1.4** | **+19.4** | **+22.8** |
| **1-OEt** | −531.5562 | −531.5542 | −531.5229 | −531.5172 | **+1.3** | **+20.9** | **+23.2** |
| **2-OMe** | −570.8434 | −570.8409 | −570.8100 | −570.8062 | **+1.6** | **+19.4** | **+21.8** |
| **3-OMe** | −803.0056 | −803.0029 | −802.9728 | −802.9687 | **+1.7** | **+20.6** | **+21.5** |
| **4-OMe** | −1116.1001 | −1116.0958 | −1116.0676 | −1116.0554 | **+2.7** | **+20.4** | **+25.4** |

Gibbs free energy values (Hartrees). Gibbs free energy differences (bold values) are in kcal/mol.

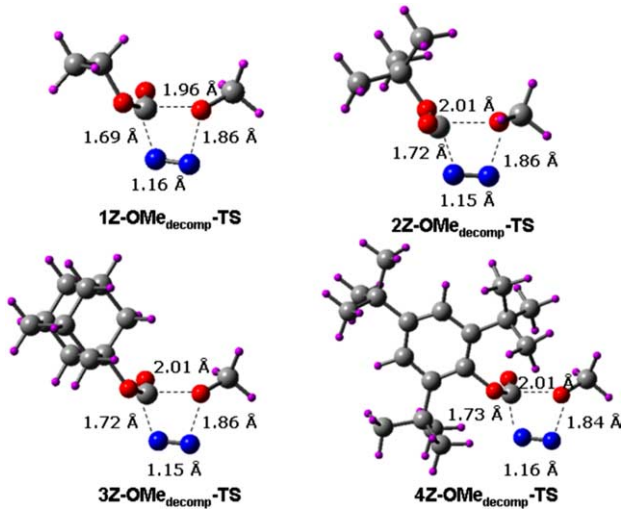


Fig. 7. Optimized transition state structures for thermal decomposition of compounds (**1Z–4Z**)-**OMe**.

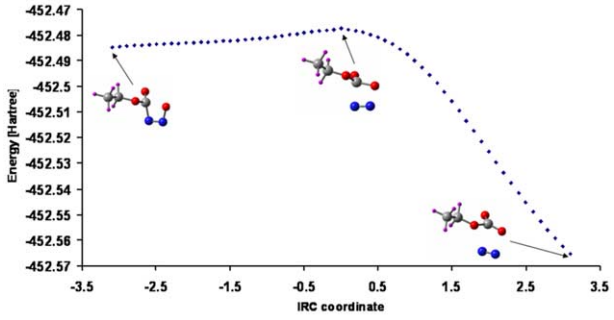


Fig. 8. An IRC profile of **1Z$_{decomp}$-TS**, with 31 steps in each direction. Data from a B3LYP/6-31+G(d)//B3LYP/6-31+G(d) calculation.

the heterolytic cleavage process is an endothermic reaction, with $\Delta G \sim +25$ kcal/mol.

### 3.2. Alkylation of the anions *1–4*

The anions of secondary *N*-nitrosocarbamates are ambident nucleophiles, with multiple alkylation sites. They can be considered, to some approximation, as the nitrogen analogs of enolate anions. However, the replacement of carbon by nitrogen brings about an important difference in the shape and nature of the HOMO, as illustrated in Fig. 9 for anion **1E** and the acetone enolate anion **5**.

The HOMO of an enolate ion, such as **5**, is of π-type, perpendicular to the σ-bond frame, whereas the HOMO of an *N*-nitrosocarbamate ion is essentially composed of n-orbitals within the N–N–O fragment, and is coplanar with the σ-bond frame. At the same time there are certain similarities: (1) NBO analysis shows that negative charge distribution is nearly equal at the *N*- and *O*-alkylation sites of **1E** or the *C*- and *O*-alkylation sites of **5**, but with a slightly greater magnitude at the N- or C-position correspondingly; (2) *N*-alkylation of **1E** and *C*-alkylation of **5** are more exothermic than *O*-alkylation, due to greater strength of the N=O vs. N=N bond or the C=O vs. C=C bond. The result is particularly surprising for anion **5** and in great contrast to earlier computational studies of enolate ions (HF/3-21G and HF/4-31G). Those studies concluded that *O*-alkylation occurred with considerably lower barrier, irrespective of the greater thermodynamic preference for *C*-alkylation [30,31]. As a result, the inherent preference for *O*-alkylation of simple enolates has come to be considered as an established fact [32].

The current analysis of the acetone enolate ion **5**, and theoretical results on its *C*- and *O*-methylation reactions (Table 6), differ significantly from those earlier conclusions. Our data suggest only slight preference for *O*-methylation with the harder electrophile $CH_3Cl$, and a preferred *C*-methylation with the softer $CH_3Br$. In the case of anion **1E**, both charge distribution and thermodynamics suggest an inherently predominant *N*-alkylation in the absence of steric factor. Replacing $CH_3Cl$ with $CH_3Br$ as the electrophile leads to a predicted slight increase of the share of *N*-alkylation, but the change is not as pronounced as in the case of anion **5**.

The calculations are in good agreement with the experimental results. Thus, NMR analysis of alkylation reactions of **1** showed *N*/*O*-alkylation ratios of 80:20 for methylation at 0 °C ($CH_3I$) and 50:50 for ethylation at 20 °C ($C_2H_5I$) [6]. The calculated ratios of rate constants for *N*-methylation ($k_N$) and *O*-methylation ($k_O$), based on our current data, are $k_N/k_O$ = 90:10 for methylation with $CH_3Cl$ (at 0 °C), $k_N/k_O$ = 95:5 for methylation with $CH_3Br$ (at 0 °C), and $k_N/k_O$ = 62:38 for ethylation with $CH_3CH_2Cl$ (at 20 °C). Increasing the size of the alkyl halide does increase the percentage of *O*-alkylation.

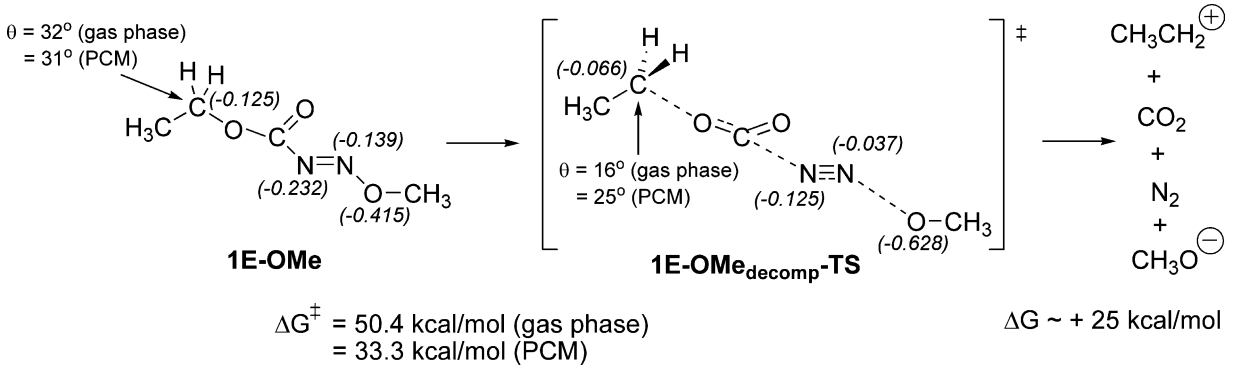


Scheme 3.

Table 5
Selected bond lengths (in Å) in the optimized structures of **1E-OMe** and **1E-OMe$_{decomp}$-TS**, in the gas phase and in solution (IEF-PCM model, solvent = acetonitrile, radii = UFF)

| Bond | 1E-OMe | | 1E-OMe$_{decomp}$-TS | |
|---|---|---|---|---|
| | Gas phase | PCM | Gas phase | PCM |
| C(H$_3$)–C(H$_2$) | 1.52 | 1.51 | 1.48 | 1.49 |
| C(H$_2$)–O | 1.46 | 1.46 | 1.92 | 1.60 |
| O–C | 1.33 | 1.33 | 1.21 | 1.23 |
| C=O | 1.21 | 1.22 | 1.17 | 1.16 |
| C–N | 1.44 | 1.44 | 2.36 | 2.14 |
| N=N | 1.23 | 1.24 | 1.12 | 1.13 |
| N–O | 1.37 | 1.36 | 2.18 | 2.14 |
| O–C(H$_3$) | 1.44 | 1.45 | 1.37 | 1.39 |

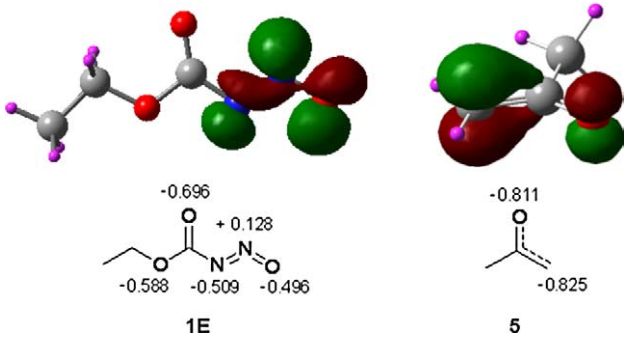


Fig. 9. HOMOs and NBO charge distributions for anion **1E** and acetone enolate anion **5**.

Large and branched carbamate groups, as in the case of **4E**, are also expected to lead to predominant *O*-alkylation, even with small electrophiles.

Additional point of concern is presented by the potentially competitive alkylation of the *E*- and *Z*-isomers of an *N*-nitrosocarbamate anion. N-alkylation, whether of the *E*- or *Z*-isomer, leads to the generation of easily interconvertible conformers, while O-alkylation gives distinct *E*- and *Z*-isomers (**1**–**4**)-**OR**, which are almost isoenergetic but separated by a large barrier for interconversion (Table 4). Experimental studies of **1** showed that in alkylation reactions with several alkyl halides, a single *O*-alkylated product was formed in each case [6]. This result is supported by our calculations. According to data in Table 2, barriers for *O*-alkylation of **1Z** are actually lower than those for **1E**. However, **1Z** is positioned unfavorably thermodynamically, being 5.8 kcal/mol higher in energy than **1E** (Fig. 10). The barrier for *E*–*Z* interconversion is low, making possible the application of the Curtin–Hammett principle. Hence the ratio *E*/*Z* of *O*-alkylation products will depend only on the difference in energies of the transition states for the two alkylation pathways ($G_Z^{\#} - G_E^{\#}$). The calculated differences $G_Z^{\#} - G_E^{\#}$ in the case of anion **1** are 3.3 kcal/mol for *O*-methylation, 2.5 kcal/mol for *O*-ethylation and 3.9 kcal/mol for *O*-isopropylation, which in turn corresponds to 0.23% **1Z-OMe**, 1.0% **1Z-OEt** and 0.076% **1Z-OPr** being present at 0 °C. Such quantities are certainly beyond NMR detection or isolation.

## 4. Conclusions

The current article represents the first attempt for a systematic theoretical analysis of secondary *N*-nitrosocarbamate anions, a class of relatively unknown ambident nucleophiles. All results are from DFT calculations, using the B3LYP functional, with a 6-31+G(d) basis set. Data have been reported on four *N*-nitrosocarbamate anions, including optimized minima structures, conformational analysis and thermal decomposition studies. Results indicate the existence of an *E*–*Z* isomer pair in each case, with relative stabilities depending on the counter ion. The *E*- and *Z*-isomer interconvert by an interesting double pyramidal inversion at the two N-centers. Thermal decomposition studies point to a concerted process, via four-membered cyclic transition state. Only the very bulky 2,4,6-tris(*t*-butyl)phenyl group seems to have an effect on the barrier of decomposition, increasing it by ~1 kcal/mol, in agreement with experimentally observed greater thermal stability of **4** compared to **1**.

Detailed analysis of alkylation reactions of anions **1**–**4** has shown that *N*-alkylation is the preferred mode of reaction in the case of small electrophiles and small carbamate substituents. *O*-alkylation receives preference with large alkyl halides or

Table 6
Results for *C*- vs. *O*-alkylation of acetone enolate anion **5** and *N*- vs. *O*-alkylation of anion **1E**

| Anion | Alkyl halide | Pre-TS **ΔG** | TS **ΔG$^{\#}$** | Post-TS **ΔG** | Pre-TS **ΔG** | TS **ΔG$^{\#}$** | Post-TS **ΔG** |
|---|---|---|---|---|---|---|---|
| **5** | | | *C*-methylation | | | *O*-methylation | |
| | CH$_3$Cl | −692.6234 | −692.6132 | −692.6951 | −692.6215 | −692.6123 | −692.6544 |
| | | **−1.9** | **+6.4** | **−45.0** | **−0.8** | **+5.8** | **−20.6** |
| | CH$_3$Br | −2804.1497 | −2804.1449 | −2804.2266 | −2804.1522 | −2804.1430 | −2804.1845 |
| | | **−4.2** | **+3.0** | **−48.3** | **−5.8** | **+5.8** | **−20.3** |
| 1E | | | *N*-methylation | | | *O*-methylation | |
| | CH$_3$Cl | −952.5608 | −952.5399 | −952.5793 | −952.5607 | −952.5379 | −952.5572 |
| | | −1.1 | +13.1 | −12.7 | −1.1 | +14.5 | +1.3 |
| | CH$_3$Br | −3064.0878 | −3064.0703 | −3064.1120 | −3064.0674 | −3064.0674 | −3064.0870 |
| | | −3.8 | +11.0 | −19.0 | −3.8 | +12.8 | −3.3 |

Gibbs free energy values (Hartrees). Gibbs free energy differences (bold values) are in kcal/mol. **ΔG** values for pre- and post-transition state minima referred to the sum energy of anion **5** (or **1E**) and CH$_3$Cl or CH$_3$Br, respectively.

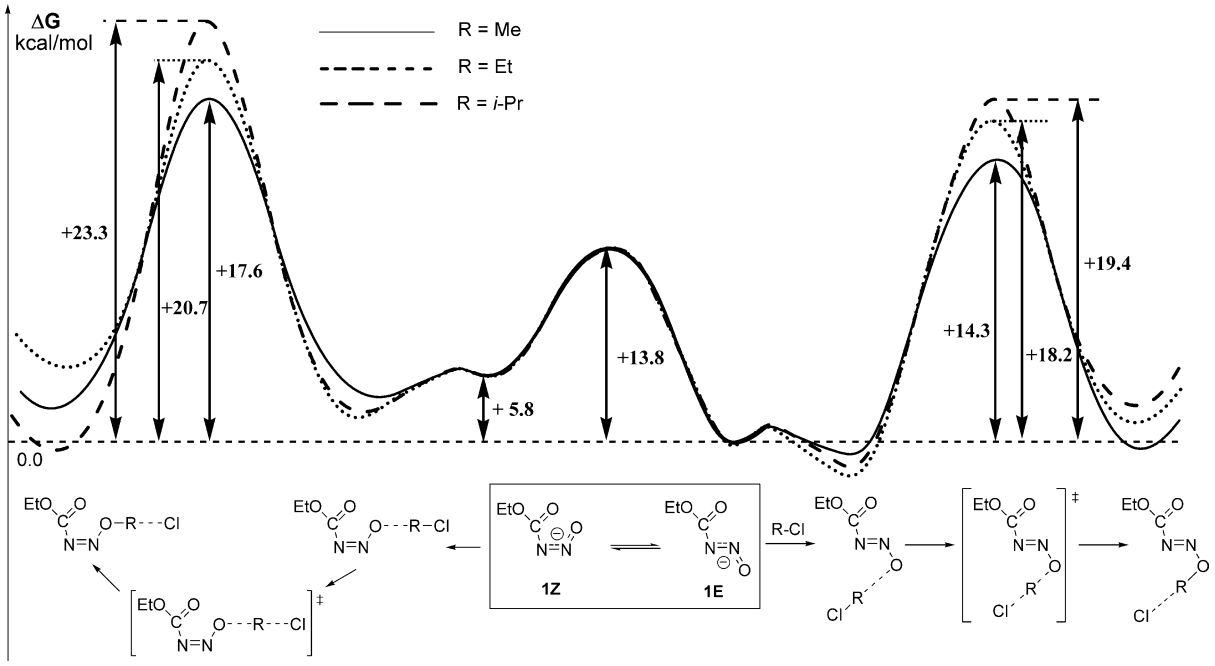


Fig. 10. Gibbs free energy profiles of several *O*-alkylation reactions of anions **1E** and **1Z**. Gibbs free energy differences (kcal/mol). All values relative to the Gibbs free energy of anion **1E**. Data from B3LYP/6-31+G(d)//B3LYP/6-31+G(d) calculations.

bulky and branched carbamate substituents. Potential competition of *E*- and *Z*-isomer alkylation has been ruled out, on the basis of lower thermodynamic stability of the *Z*-isomers and application of the Curtin-Hammett principle.

The synthetically desirable (and challenging) *O*-alkylation products have been analyzed as well, the results indicating that they too exist as pairs of *E*- and *Z*-isomers, which are almost isoenergetic and related by relatively large interconversion barriers. The *O*-alkylated derivatives are expected to be thermally unstable, but less so than the parent anions, particularly the derivatives of anion **4**. Our results indicate that compounds such as **4-OMe** would have enhanced thermal stability that should facilitate their isolation and characterization.

## Acknowledgements

Partial funding for this work was provided by the University of Dayton Research Council.

## Supplementary data

Supplementary data associated with this article can be found, in the online version, at doi:10.1016/j.theochem.2006.01.030.

## References

[1] T.K. Rao, W. Lijinsky, J.L. Epler, Genotoxicology of *N*-Nitroso Compounds, Plenum Press, New York, 1984.
[2] G.P. Wheeler, B.J. Bowdon, J.A. Grimsley, H.H. Lloyd, Cancer Res. 34 (1974) 194–200.
[3] G.A. Digenis, C.H. Issidorides, Bioorg. Chem. 8 (1979) 97–137.
[4] V. Gadjeva, Eur. J. Med. Chem. 37 (2002) 295–300.
[5] J. Thiele, A. Lachman, Justus Liebigs Ann. Chem. 288 (1895) 304–311.
[6] V. Benin, P. Kaszynski, G. Radziszewski, J. Am. Chem. Soc. 124 (2002) 14115–14126.
[7] A. Thakkalapally, V. Benin, Tetrahedron 61 (2005) 4939–4948.
[8] M.J. Frisch, G.W. Trucks, H.B. Schlegel, G.E. Scuseria, M.A. Robb, J.R. Cheeseman, J.A. Montgomery Jr., T. Vreven, K.N. Kudin, J.C. Burant, J.M. Millam, S.S. Iyengar, J. Tomasi, V. Barone, B. Mennucci, M. Cossi, G. Scalmani, N. Rega, G.A. Petersson, H. Nakatsuji, M. Hada, M. Ehara, K. Toyota, R. Fukuda, J. Hasegawa, M. Ishida, T. Nakajima, Y. Honda, O. Kitao, H. Nakai, M. Klene, X. Li, J.E. Knox, H.P. Hratchian, J.B. Cross, V. Bakken, C. Adamo, J. Jaramillo, R. Gomperts, R.E. Stratmann, O. Yazyev, A.J. Austin, R. Cammi, C. Pomelli, J.W. Ochterski, P.Y. Ayala, K. Morokuma, G.A. Voth, P. Salvador, J.J. Dannenberg, V.G. Zakrzewski, S. Dapprich, A.D. Daniels, M.C. Strain, O. Farkas, D.K. Malick, A.D. Rabuck, K. Raghavachari, J.B. Foresman, J.V. Ortiz, Q. Cui, A.G. Baboul, S. Clifford, J. Cioslowski, B.B. Stefanov, G. Liu, A. Liashenko, P. Piskorz, I. Komaromi, R.L. Martin,D.J. Fox, T. Keith, M.A. Al-Laham C.Y. Peng, A. Nanayakkara, M. Challacombe, P.M.W. Gill, B. Johnson, W. Chen, M.W. Wong, C. Gonzalez, J.A. Pople, GAUSSIAN 03, Gaussian, Inc., Wallingford, CT, 2004.
[9] Parallel Quantum Solutions, 2013 Green Acres Road, Suite A, Fayetteville, Arkansas 72703.
[10] A.D. Becke, Phys. Rev. A 38 (1988) 3098–3100.
[11] C. Lee, W. Yang, R.G. Parr, Phys. Rev. B 37 (1988) 785–789.
[12] M.J. Frisch, J.A. Pople, J.S. Binkley, J. Chem. Phys. 80 (1984) 3265–3269.
[13] J. Chandrasekhar, J.G. Andrade, P.V.R. Schleyer, J. Am. Chem. Soc. 103 (1981) 5609–5612.
[14] G.W. Spitznagel, T. Clark, J. Chandrasekhar, P.V.R. Schleyer, J. Comput. Chem. 3 (1982) 363–371.
[15] T. Clark, J. Chandrasekhar, G.W. Spitznagel, P.V.R. Schleyer, J. Comput. Chem. 4 (1983) 294–301.
[16] G.W. Spitznagel, T. Clark, P.V.R. Schleyer, W.J. Hehre, J. Comput. Chem. 8 (1987) 1109–1116.
[17] C. Gonzalez, H.B. Schlegel, J. Chem. Phys. 90 (1989) 2154.
[18] C. Gonzalez, H.B. Schlegel, J. Chem. Phys. 94 (1990) 5523.

[19] C. Peng, H.B. Schlegel, Israel J. Chem. 33 (1994) 449.
[20] C. Peng, P.Y. Ayala, H.B. Schlegel, M.J. Frisch, J. Comput. Chem. 17 (1996) 49.
[21] M.T. Cances, B. Mennucci, J. Tomasi, J. Chem. Phys. 107 (1997) 3032–3041.
[22] B. Mennucci, J. Tomasi, J. Chem. Phys. 106 (1997) 5151–5158.
[23] M. Cossi, V. Barone, B. Mennucci, J. Tomasi, Chem. Phys. Lett. 286 (1998) 253–260.
[24] P. Haberfield, P.M. Block, M.S. Lux, J. Am. Chem. Soc. 97 (1975) 5804–5806.
[25] W.A. Sokalski, R.W. Gora, W. Bartkowiak, P. Kobylinski, J. Sworakowski, A. Chyla, J. Leszczynski, J. Chem. Phys. 114 (2001) 5504–5508.
[26] T.H. Lowry, K.S. Richradson, Mechanism and Theory in Organic Chemistry, Harper & Row, New York, NY, 1987.
[27] V. Benin, Unpublished results.
[28] R.W. Darbeau, R.S. Pease, R.E. Gibble, J. Org. Chem. 66 (2001) 5027–5032.
[29] R.W. Darbeau, E.V. Perez, J.I. Sobieski, W.A. Rose, M.C. Yates, B.J. Boese, N.R. Darbeau, J. Org. Chem. 66 (2001) 5679–5686.
[30] K.N. Houk, M.N. Paddon-Row, J. Am. Chem. Soc. 108 (1986) 2659–2662.
[31] S. Damoun, G. Van de Woude, K. Choho, P. Geerlings, J. Phys. Chem. A 103 (1999) 7861–7866.
[32] S.S. Shaik, H.B. Schlegel, S. Wolfe, Theoretical Aspects of Physical Organic Chemistry: The $S_N2$ Mechanism, Wiley, New York, NY, 1992.